

UNDERSTANDING THE ALCHEMILLA LEAF AND ITS  
HYDROPHOBICITY

by

ATUL MOHANDAS KOOTATHIL

Presented to the Faculty of the Graduate School of

The University of Texas at Arlington

In Fulfillment of Requirements for the Degree of

MASTER OF SCIENCE IN MECHANICAL ENGINEERING

THE UNIVERSITY OF TEXAS AT ARLINGTON

MAY 2016

Copyright © by Dr. Cheng Luo's Group 2016

All Rights Reserved



## Acknowledgement

I take this opportunity to convey my immense gratitude and respect for my thesis advisor and committee chair, Dr. Cheng Luo, who through his expertise has been an excellent guide and patient motivator on my road to become an independent researcher. The skill and knowledge gained through this experience has made an impact on my overall betterment and growth as an individual. I extend my sincerest thanks to my thesis committee members Dr. Hyejin Moon and Dr. Zhen Xue Han, who took out time to guide me through my research work.

May 03, 2016

## Dedication

I dedicate the thesis to my family who have been a constant source of support and encouragement.

May 03, 2016

## Abstract

### UNDERSTANDING THE ALCHEMILLA LEAF AND ITS HYDROPHOBICITY

Atul Mohandas Kootathil, MS

The University of Texas at Arlington, 2016

Supervising Professor: Dr. Cheng Luo

The Alchemilla leaf has been well known and studied frequently for its hydrophobic ability. However, much difficulty has been met in replicating its microstructure for hydrophobic applications. Also, not much experimental data was found on the behavior of leaf's microstructure. Gathering information from experimental results may provide new understanding of its wetting properties before attempting to mimetic its wetting behavior. In this research, the focus is to detail the observed solid-water-air interaction on Alchemilla leaf by simulating condensation, evaporation and rainfall conditions, which are the common ways that a plant may interact with water drops in nature. Documenting these observations sheds light on the different ways that the surface structures of Alchemilla leaf interact with water drops.

## Table of Contents

Acknowledgement .....	iii
Abstract .....	v
List of Figures .....	vii
List of Tables.....	ix
Chapter 1 Introduction .....	1
Chapter 2 Experimental Setup .....	3
Chapter 3 Results and Discussion .....	5
3.1. Structure of Alchemilla Leaf.....	5
3.2. Pressing Test .....	7
3.3. Water-IPA mixture drop test .....	12
3.4. Contact Angle and Tilt Angle Measurement.....	13
3.5. Condensation Experiment .....	23
3.6. Evaporation Experiment.....	28
3.7. Rain Drop Experiment .....	31
3.8. Self-Cleaning Ability Experiment.....	32
Chapter 4 Summary and Future Work .....	33
References.....	34
Biographical Information.....	36

## List of Figures

- Figure 1.** Alchemilla leaf structures: (a) overview of part of a leaf (optical image), and close-up views of fibers that are located (b) near the center and (c) close to margin of the leaf (SEM images). ..... 6
- Figure 2.** Pressing test on an untreated Alchemilla leaf: (a) effect of fibers on drop and (b) effect of leaf surface on drop. Arrow represents the direction of motion of drop. .... 11
- Figure 3.** Pressing test on a Telfon-coated Alchemilla leaf. .... 11
- Figure 4.** Pressing test on a Hydrobead-coated Alchemilla leaf. .... 11
- Figure 5.** Drop of water-IPA mixture on leaf having concentration (a) 0%, (b) 10%, (c) 20%, (d) 30%, (e) 35% and, (f) 40% of IPA. (C.A. = contact angle with the leaf face).. 12
- Figure 6.** (a) Water drop condensed on fiber. Advancing and receding contact angles measured at 85° tilt for (b) water drop on an untreated leaf, (c) water-IPA drop on untreated leaf, (d) water drop on Teflon-coated leaf and (e) water drop on Hydrobead-coated leaf. .... 17
- Figure 7.** Graph plot comparing average drop volume for different cases against tilt angle..... 19
- Figure 8.** Illustration of cases in condensation processes: (a) drop on a single fiber, (b) drop suspended between multiple fibers and (c) merger of drop on fiber with drop on leaf face..... 25
- Figure 9.** Condensation of drops on (a) a single fiber and (b) a group of fibers..... 26

**Figure 10.** (a) The drops marked within circle 1 and 2 merged to form bigger drops 1' and 2', respectively. (b) Movement of fibers during a condensation process. (c) Pinning effect observed due to closely packed fibers at margin of a leaf. .... 27

**Figure 11.** Evaporation of (a) drops on a single fiber and between two fibers and (b) a large drop having contact with multiple fibers and the leaf face. .... 30

**Figure 12.** Splitting of a small drop during an evaporation process. .... 30

**Figure 13.** (a1) A water drop was poured on a leaf using a micropipette and (a2) no water residue was visibly seen after the drop rolled off the leaf. (b1) Water drops were condensed on the leaf and (b2) no water residue visibly seen after the larger drops carried the smaller drops as they rolled off the leaf. .... 31

**Figure 14.** Optical images demonstrating self-cleaning ability: Top view of (a1) leaf with particles, and (a2) clean leaf face after drop rolled off. Side view of (b1) particles with diameters in the range of 5 – 500  $\mu\text{m}$ , and (b2) clean leaf face with traces of particles of diameters  $<10\mu\text{m}$  after the drop rolled off. .... 32



## List of Tables

<b>Table 1.</b> Comparison of average drop volume for different cases against fixed tilt angles. All volumes measured lie within an error of 1 $\mu$ L. ....	18
<b>Table 2.</b> Variations of receding contact angle, advancing contact angle, and tilt angles with drop volumes for Alchemilla leaf. All angles and volumes measured lie within an error of 2 $^{\circ}$ and 1 $\mu$ L, respectively. ....	20
<b>Table 3.</b> Variations of advancing and receding contact angle for water-IPA drop on untreated Alchemilla leaf. All angles and volumes measured lie within an error of 2 $^{\circ}$ and 1 $\mu$ L, respectively. ....	21
<b>Table 4.</b> Variations of advancing and receding contact angles for Teflon-coated Alchemilla leaf. All angles and volumes measured lie within an error of 2 $^{\circ}$ and 1 $\mu$ L, respectively. ....	21
<b>Table 5.</b> Variations of advancing and receding contact angles for Hydrobead-coated Alchemilla leaf. All angles and volumes measured lie within an error of 2 $^{\circ}$ and 1 $\mu$ L, respectively. ....	22

## Chapter 1

### Introduction

Nature has constantly been a source of inspiration towards understanding and designing new methods to create artificial hydrophobic materials [1]-[3]. This hydrophobic property observed with plants (Lotus, *Alchemilla*, etc.) and animals (Namib Desert beetle) is an outcome of evolution. The Lotus leaf has hydrophobic, hierarchal micro/nanopillars which allow easy rolling of water drops and give it self-cleaning ability [4]. In contrast to Lotus, the leaf of the *Alchemilla mollis* has a dense cover of fibers which grant it hydrophobicity. After rain the *Alchemilla* leaf can be spotted to remain dry with some spherical water drops on it. On a misty morning, spherical water drops are found at the leaf margins which is formed by the process of guttation. Guttation is process by which internal water is forced out of hydathodes located at the leaf margin [9]. Guttation is believed to have a role in protecting the plant from grazing animals and pathogens. It is normally easy to form spherical drops on hydrophobic surfaces than on hydrophilic surfaces, due to the material having low wetting. However, the fibers of *Alchemilla* leaf are hydrophilic. Otten and Herminghaus[3] proposed that such drops were formed due to support of flexible fiber clusters on the leaf face which form due to capillary forces. An attempt was made at replicating this behavior on artificial surface (PHEMA) which was unsuccessful, since water got incorporated between the micro structures [7]. It was later experimentally demonstrated that there is neither clustering nor bending of fibers due to capillary forces. A theoretical approach also discussed the difficulty of capillary interaction overcoming elastic forces for the formation of spherical drops [6]. A recent investigation of conical hair fibers on the leg of water strider has demonstrated the role of its hydrophobic hair fibers in expelling water

drops on its leg, allowing it to stay afloat on water [8]. The fibers on the Alchemilla leaf could play a similar role to form spherical water drops on the leaf.

Our goal is to understand through experimentation the role of fibers on the Alchemilla leaf and examine its self-cleaning ability. By gathering thorough understanding of the mechanism on Alchemilla leaf it gives us better potential when attempting to mimetic its wetting properties on artificial materials.

## Chapter 2

### Experimental Setup

**Sample Preparation.** A fresh cut leaf of the *Alchemilla mollis* was cleaned with deoxidized water and air dried to remove any foreign particles before using them to perform experiments.

**Scanning Electron Microscopy.** The initial analysis of a fresh leaf sample was done using an optical microscope. Further analysis was conducted under a scanning electron microscope (SEM), first with an uncoated leaf sample. Then a specimen was sputter coated with silver for 30 seconds to obtain clearer images of the leaf.

**Pressing Test.** Pressing test was conducted on the *Alchemilla* leaf to determine the wetting states on its microstructure. For the test, a water drop of volume 2 $\mu$ l was placed on a glass slide coated with Hydrobead (contact angle >150 $^{\circ}$ ), then pressed against the leaf sample, and allowed to slowly separate from the leaf. The same procedure was then performed on leaf samples coated with Teflon and Hydrobead, each.

**Water-IPA test.** A leaf sample was setup under the optical microscope and a 2 $\mu$ l drop of distilled water and isopropyl alcohol (IPA) mixture was placed on it. The concentration of IPA in the mixture was increased until the drop collapsed on the leaf.

**Contact Angle and Tilt Angle Measurement.** A leaf sample was placed on a glass slide under the optical microscope and a humidifier (Air-o-Swiss 7135 Ultrasonic, Boneco USA Co.) was used to condense small water drops on its fibers. For the tilt test, glass slide with samples of untreated, Teflon-coated and Hydrobead-coated *Alchemilla* leaf were lifted up from one end and set at fixed tilt angles. A water or water-IPA mixture drop was then placed on it using a

micropipette (Eppendorf, Physiocare Concept) and its volume was increased by 2 $\mu$ l until it rolled or slipped off.

**Condensation and Evaporation Experiments.** The leaf sample was fixed on a glass slide, and a humidifier was used to direct water vapor on the leaf. The camera (Digital Microscope, Dino-Lite Pro) was set up to take pictures and videos and a stop watch used to measure time intervals. The same setup was then prepared under an optical microscope and recorded for detailed observation.

**Rain Drop Experiment.** Two dry leaf samples, one on which water vapor was allowed to condense and other where water was poured using a pipette were compared to determine possibility of air entrapment under the water drops.

**Self-cleaning Ability Experiment.** The leaf sample was sprinkled with particles of sizes less than 500 $\mu$ m. Drops of water were poured using a pipette and allowed to roll down the leaf sample, to observe whether the leaf had self-cleaning ability.

## Chapter 3

### Results and Discussion

#### 3.1. Structure of Alchemilla Leaf

The leaf is covered with fibers having lengths ' $l$ ' in the range of 400 to 800  $\mu\text{m}$  (Figure 1.a). While most of them were around 500 $\mu\text{m}$  long, the longer fibers were found at the margin of the leaf. The gap ' $a$ ' between two fibers ranges from 150 – 220  $\mu\text{m}$  (Figure 1.b) with the exception of the dense cluster at the margin of the leaf, whose gap is around 50 $\mu\text{m}$  (Figure 1.c). The diameter ' $d$ ' of fibers were around 8 – 15  $\mu\text{m}$  at the base and tapered to the apex to around 3 – 6  $\mu\text{m}$ . Most fibers on the leaf were observed to incline toward the margin of the leaf but at varying angles. The fibers close to the margins had inclinations of  $<20^\circ$  and the fibers on the rest of the leaf had inclinations varying from around  $30^\circ$ - $90^\circ$ . Apart from the inclination, many fibers were observed to overlap and cross each other at random. Therefore, it should not to be assumed to be a neatly brushed pattern throughout the length of the leaf. The leaf face has a waxy, cell structure as visible in SEM image (Figure 1.c).

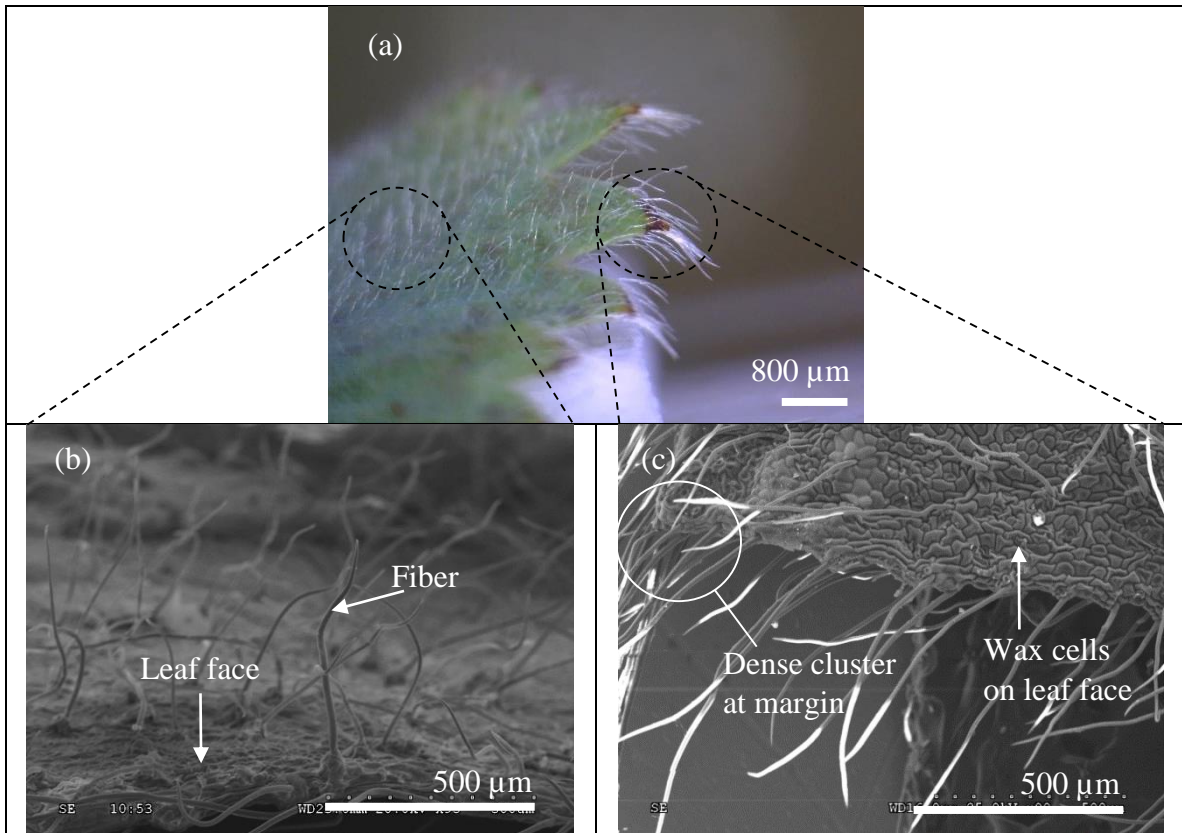


**Figure 1.** Alchemilla leaf structures: (a) overview of part of a leaf (optical image), and close-up views of fibers that are located (b) near the center and (c) close to margin of the leaf (SEM images).

## 3.2. Pressing Test

### 3.2.1. Untreated Alchemilla leaf

The pressing test was conducted in two parts, one highlighting the influence of fibers (Figure 2.a), and other the influence of leaf face (Figure 2.b) on the water drop. In Figure 2.a, the fibers can be observed to penetrate the drop as it was slowly pressed closer to the leaf face. During separation, the water profile was slightly pulled by the fibers which is marked by circle in Figure 2.a6. On pressing the drop until it reached leaf face (Figure 2.b), it was observed that the water drop gets elongated while separating from the leaf face. After separation, some traces of water or residual drops were found between fibers that crossed each other.

In the pressing test, the advancing angle and receding contact angle for a single fiber were measured at around  $90^\circ$  and in the range of  $70^\circ - 80^\circ$ , respectively (Figure 2.a) and for leaf face they were measured in the range of  $140^\circ - 150^\circ$  and  $110^\circ - 120^\circ$ , respectively (Figure 2.b). Comparing Figures 2.a4 and 2.a5, we observe an amplification in the receding angle when drop is influenced by a group of fibers. Therefore, the receding and advancing contact angle of drop on the microstructure will be determined by the cumulative effect of fibers and leaf face interacting with it.

The microstructure of the Alchemilla is similar to the PDMS microstructure that was used to determine the angle inequality in for intermediate states between transition from Cassie-Baxter to Wenzel state. The Eqn. (1) stated below was established to be the necessary condition for a water drop to exist in an intermediate state on the microstructure [5].

$$360^\circ < (\theta_{01} + \theta_{02} + \varphi) \quad (1)$$



where,  $\theta_{01}$ ,  $\theta_{02}$ , and  $\varphi$  denotes angle made by water drop with leaf face, contact angle of water drop with fiber, and angle between fiber and leaf face, respectively.

Contact angle of water drop with fiber in our observations were approximately  $90^\circ$ . Considering  $\theta_{02} \sim 90^\circ$ , the Eqn. (1) reduces to the condition that for all  $(\theta_{01} + \varphi) < 270^\circ$  the drop should contact leaf face. However, if  $(\theta_{01} + \varphi) > 270^\circ$ , the drop may stay suspended on fibers. For fibers the angle of orientation varies from  $30^\circ - 90^\circ$ . On further simplification by considering  $\varphi \sim 90^\circ$ , we get for all  $\theta_{01} < 180^\circ$  the drop should contact leaf face and for all  $\theta_{01} > 180^\circ$  the drop may stay suspended on the fibers. Therefore, smaller inclination of fibers opened possibility for a meta-stable configuration which allowed water drops to stay suspended on fibers and such configuration has also theoretically satisfied conditions to achieve a low energy state in a previous study [11].

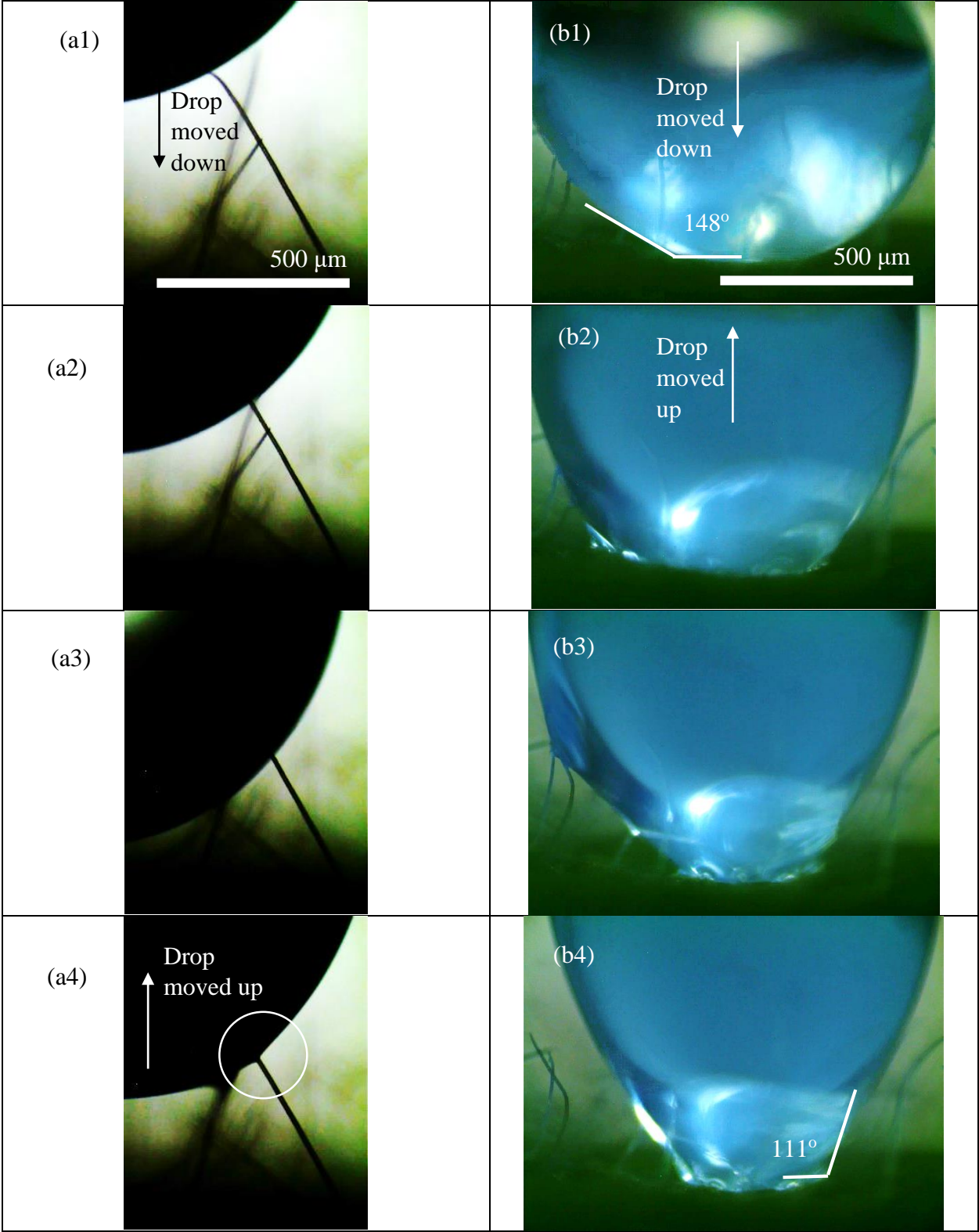
### 3.2.2. Teflon-coated Alchemilla leaf

The Alchemilla leaf was coated with Teflon or Polytetrafluoroethylene (PTFE) to determine the effect of microstructure if fibers were hydrophobic. The water drop pressed against the microstructure was observed to deform immediately on coming in contact with the fibers (Figure 3). The advancing contact angle was measured in the range of  $120^\circ - 130^\circ$ . The fibers would bend in effort to resist the drop that was being pressed on it. However, as the drop moved closer to the leaf face, the fiber finally punctured the drop and the drop came to rest on the leaf face. During separation, the drop was elongated to smaller extent compared to the drop on untreated Alchemilla leaf, which indicates pinning forces are lower. The receding contact angle was measured in the range of  $100^\circ - 110^\circ$ . There was no visible water residue on the leaf surface after separation.

### 3.2.3. Hydrobead-coated Alchemilla leaf

The pressing test was then repeated on Hydrobead-coated Alchemilla leaf. The leaf fibers had become stiff due to Hydrobead coat and directly punctured the drop pressing against it. The advancing contact angle was observed to be  $>150^\circ$ . During separation, the drop was barely elongated and the receding contact angle was  $>140^\circ$ . No visible water residue was found on the leaf surface. These observations were similar to the pressing test results of *President Lotus* [4]. It implies that the adhesion force between water and the Hydrobead-coated leaf surfaces were the weakest.

The elongation of the drop observed during separation is due to pinning force exerted by the microstructure. The above tests indicate that the pinning force experienced by the drop decrease as the fibers become more hydrophobic. These results are in agreement to our hypothesis that the waxy leaf face is the reason for the leaf's hydrophobic properties.



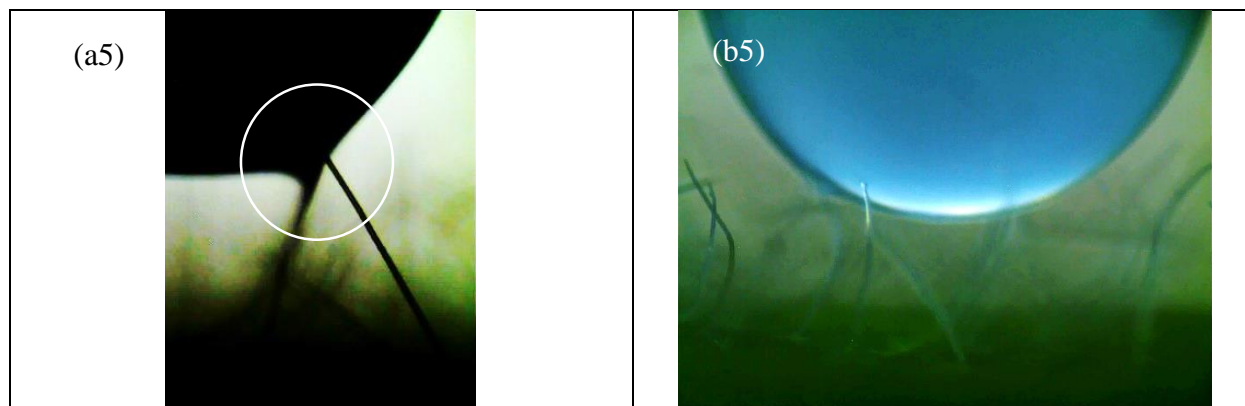


**Figure 2.** Pressing test on an untreated Alchemilla leaf: (a) effect of fibers on drop and (b) effect of leaf surface on drop. Arrow represents the direction of motion of drop.

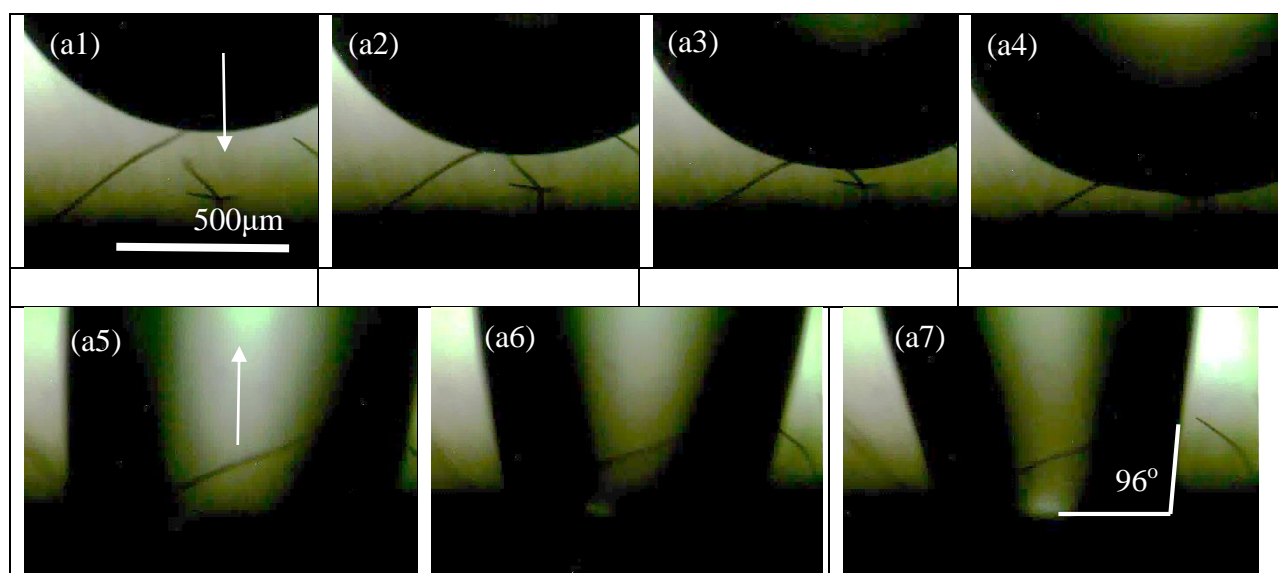


**Figure 3.** Pressing test on a Telfon-coated Alchemilla leaf.

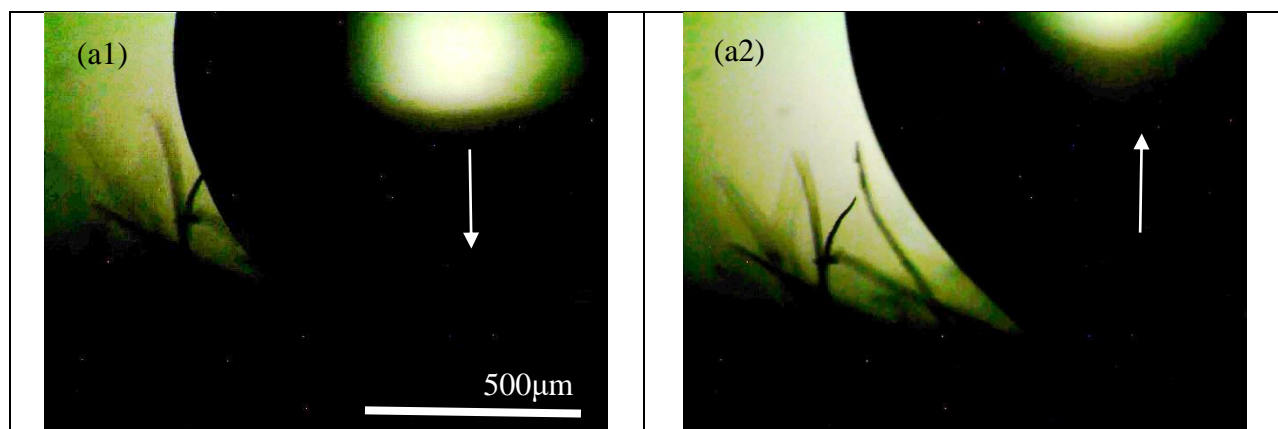


**Figure 4.** Pressing test on a Hydrobead-coated Alchemilla leaf.

### 3.3. Water-IPA mixture drop test

A 2 $\mu$ L drop of water placed on the untreated *Alchemilla* leaf was observed under microscope and its contact angle with the leaf face was measured. Then, a 2 $\mu$ L drop of water-IPA mixture was placed on the leaf and its contact angle with leaf face was recorded. The IPA concentration in the mixture was increased in steps of 10% until the drop collapsed onto the leaf face. As the IPA concentration increased, the drop became flatter on the leaf. For 40% IPA concentration, the drop was observed to collapse on the leaf face as soon as it was placed on the leaf.

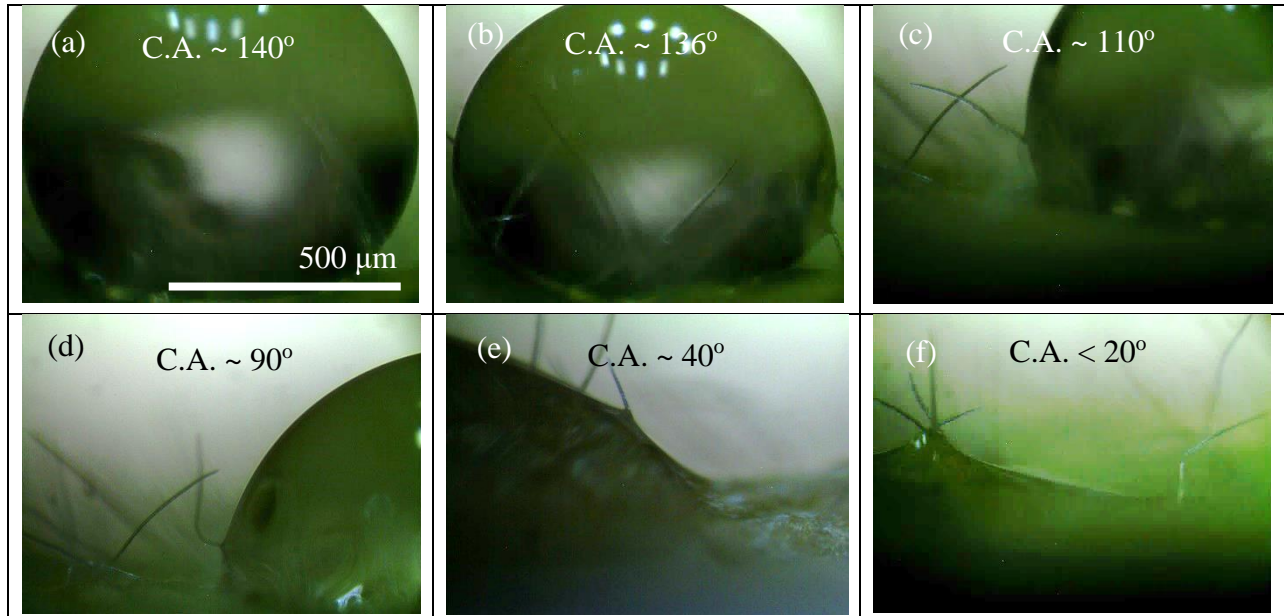


**Figure 5.** Drop of water-IPA mixture on leaf having concentration (a) 0%, (b) 10%, (c) 20%, (d) 30%, (e) 35% and, (f) 40% of IPA. (C.A. = contact angle with the leaf face).

### 3.4. Contact Angle and Tilt Angle Measurement

A preliminary contact angle test was performed to determine the nature of water interaction with fibers on Alchemilla leaf. Water vapor from humidifier was allowed to condense on the leaf sample. The clamshell-shaped water drops that were formed on fiber had contact angles in the range of  $85^\circ - 90^\circ$  (Figure 6.a).

Tilt tests were performed on the Alchemilla leaf to determine whether water drops were easy to get off from the leaf surface. It is known that the critical tilt angle (i.e., the minimum tilt angle for a drop to move down) is related to drop volume [12],[13]. A sample of Alchemilla leaf on glass slide was set at fixed tilt angles ranging from  $25^\circ - 85^\circ$  in increments of  $10^\circ$ . At each specific tilt angle we desire to measure the corresponding minimum volume of drop that would roll or slide down the leaf. To find this minimum volume, a water drop of  $2\mu\text{l}$  was placed on the tilted leaf using a micropipette, and its volume was increased in  $2\mu\text{l}$  increments until it rolled or slid down.

For the tilt test, an untreated leaf sample was tested and corresponding measurements were recorded as shown in Table 2. It was observed that the volume of drop decreased from  $52 - 22\ \mu\text{L}$  as tilt angle increased. The advancing and receding contact angles were measured for each drop and recorded (Figure 6.a). Accordingly, the contact angle hysteresis varied in the range of  $69^\circ - 87^\circ$ .

To verify these results theoretically, we look at the balance of forces on a water drop on an inclined plane,

$$mg \sin \alpha = 2\gamma r(\cos \theta_r - \cos \theta_a) \quad (2)$$

where,  $m$  denotes the mass of the drop,  $g$  gravitational acceleration,  $\alpha$  minimum tilt angle for water to move down on the plate,  $\gamma$  surface tension of water,  $r$  the radius of the drop,  $\theta_r$  receding angle, and  $\theta_a$  advancing angle. The left-hand side of Eqn. (2) is the component of gravitational force along an inclined plane and the right-hand side is the surface tension force generated due to the difference between receding and advancing angles. If  $V$  is considered to be drop volume, then  $V$  should be related to  $r$  as [14]

$$V = \frac{1}{6} \pi r^3 \tan \frac{\theta}{2} (3 + \tan^2 \frac{\theta}{2}) \quad (3)$$

where,  $\theta$  denotes contact angle which is given by Wenzel model for rough surface as,

$$\cos \theta = r \cos \theta_Y \quad (4)$$

where,  $\theta_Y$  denotes the Young's contact angle measured for the water drop on the leaf at a horizontal plane and  $r$  is the roughness ratio. It follows from Eqns. (2) and (3) that,

$$\sin \alpha = \frac{2\gamma(\cos \theta_r - \cos \theta_a)}{\rho g V^{2/3}} \left[ \frac{6}{\pi \tan \frac{\theta}{2} (3 + \tan^2 \frac{\theta}{2})} \right]^{1/3} \quad (5)$$

where,  $\rho$  denotes density of water.

The advancing and receding angles measured for water drop at different tilt angles were used in Eqn. (5) to compute  $\alpha$  for the respective drop volumes (Table 2). The theoretical results obtained were in close agreement to the experimental tilt angles. The error between the experimental and theoretical tilt angles may be due to the pinning forces which were not factored into the equations. It is also noted that, the theoretical minimum tilt angles decreased as the drop volume increased.

To establish the influence of fibers and associated pinning force on the drop we conducted tilt test using water-IPA solution on untreated leaf, water on Teflon-coated leaf and water on Hydrobead-coated leaf. The average of the measurements for minimum drop volumes recorded at each tilt angle for all of the above cases were compared side-by-side in Table 1 and represented using a graph in Figure 7.

In the second tilt test, a drop of water-IPA was placed on the untreated leaf sample used in the previous test. The minimum drop volume corresponding to small tilt angle had increased compared to the previous test. However, at large tilt angles, the volume of water-IPA drop was almost the same as the volume of water drop on the untreated leaf. The hydrophilic water-IPA drop moves down the leaf face at lower volumes because the fiber allows it to spread faster. The advancing and receding contact angles were measured at various tilt angles (Figure 6.b) and the contact angle hysteresis was calculated to vary in the range of  $54^{\circ} - 100^{\circ}$  (Table 3).

In the third tilt test, water drop was placed on a Teflon-coated leaf at varying tilt angles (Figure 6.c) and its advancing and receding contact angles were recorded in Table 4. The volumes of the drops were slightly smaller at small tilt angles and vastly smaller at large tilt angles compared to the untreated leaf. The contact angle hysteresis for the Teflon-coated leaf lie in the range of  $34^{\circ} - 62^{\circ}$ .

In the fourth tilt test, water drop was placed on a Hydrobead-coated leaf at varying tilt angles. The advancing and receding contact angles were measured and recorded (Table 5). The volumes of the drops were smallest at every tilt angle when compared to both untreated and Teflon-coated leaf. The contact angle hysteresis for the Hydrobead-coated leaf lie in the range of  $12^{\circ} - 44^{\circ}$ . At  $85^{\circ}$  tilt, the drop on the leaf was completely suspended on the fibers and had no contact with the leaf face (Figure 6.e).



The results from the hydrophobic coated leaf samples indicate that changing the nature of the fiber significantly decreased the contact angle hysteresis and had reduced the pinning force on the drop.

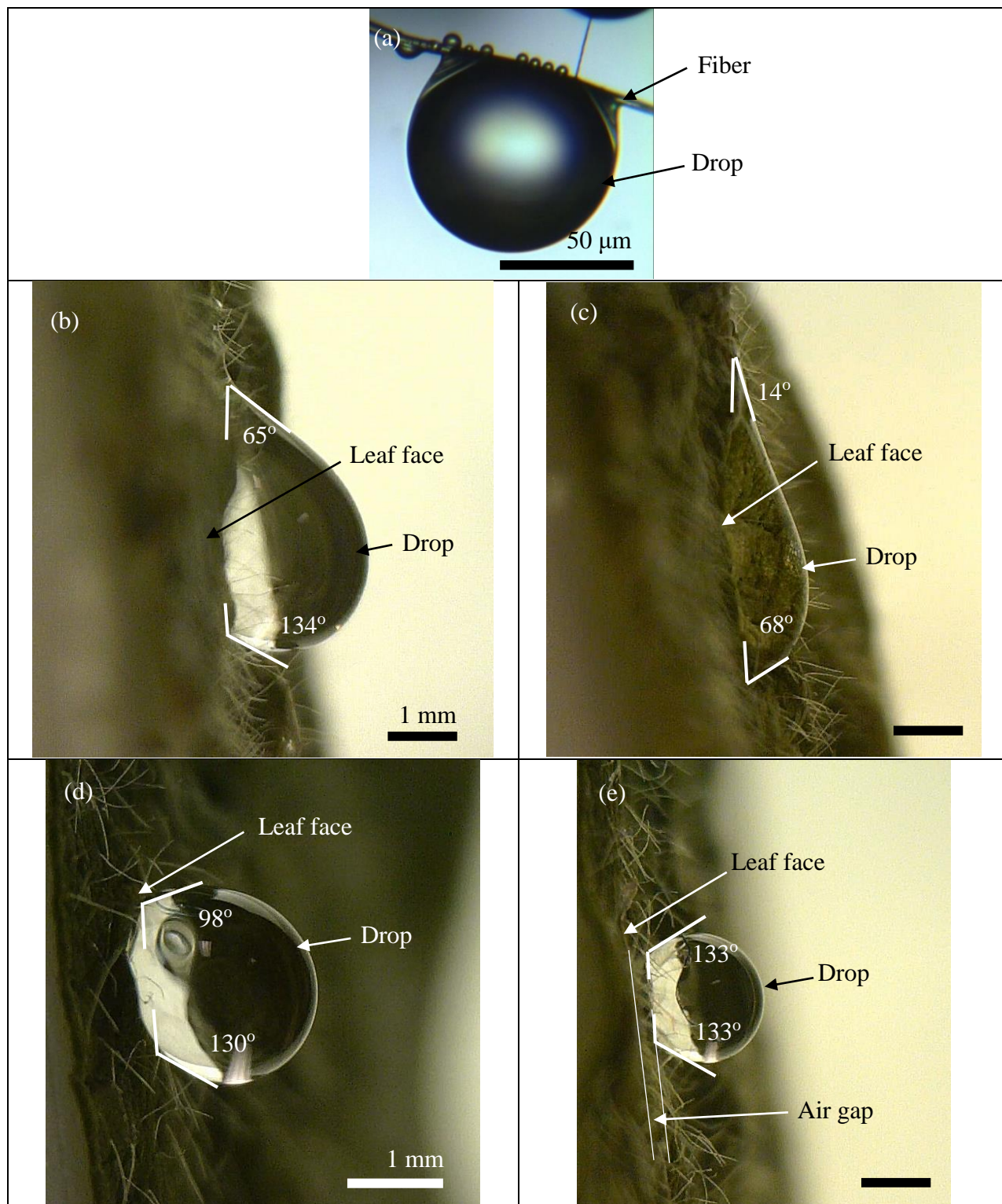


**Figure 6.** (a) Water drop condensed on fiber. Advancing and receding contact angles measured at 85° tilt for (b) water drop on an untreated leaf, (c) water-IPA drop on untreated leaf, (d) water drop on Teflon-coated leaf and (e) water drop on Hydrobead-coated leaf.

Volume ( $\mu\text{L}$ ) Tilt angle ( $^\circ$ )	Water drop on untreated leaf	Water-IPA (65:35) mixture drop on untreated leaf	Water drop on Teflon-coated leaf	Water drop on Hydrobead-coated leaf
25	51	54	49	33
35	46	49	35	22
45	35	41	25	15
55	29	35	16	8
65	25	29	13	8
75	24	21	9	4
85	21	18	6	4

**Table 1.** Comparison of average drop volume for different cases against fixed tilt angles. All volumes measured lie within an error of  $1\mu\text{L}$ .

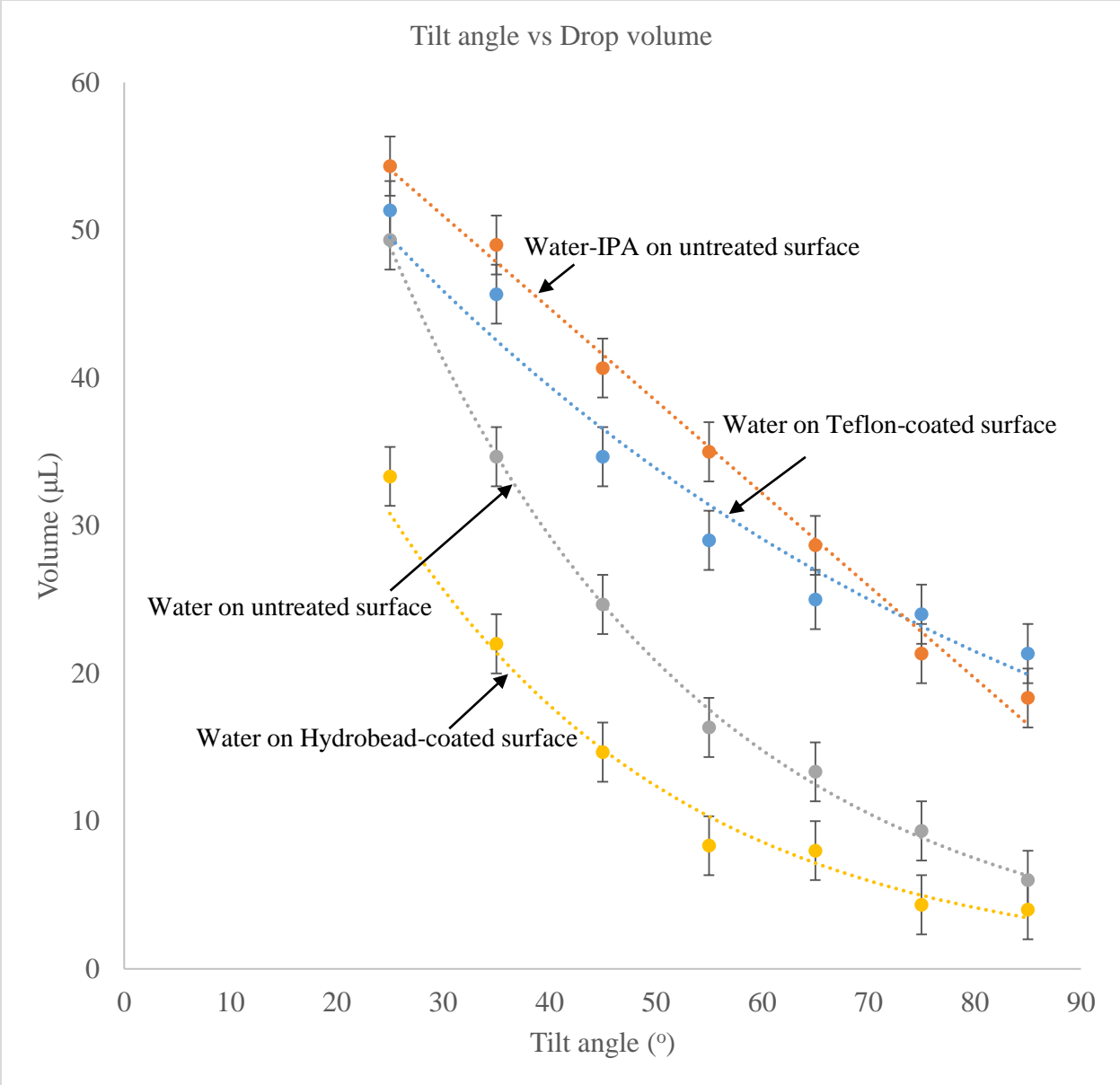


**Figure 7.** Graph plot comparing average drop volume for different cases against tilt angle.

Tilt angle (°)	Volume (μL)	Contact angle (°)		Hysteresis (°)	Tilt angle (°)
Experimental value		Advancing	Receding	Difference between advancing and receding contact angles	Theoretical value
25	52	134	65	69	28
35	44	131	47	84	39
45	34	132	46	86	50
55	28	128	48	80	55
65	26	131	45	86	67
75	24	134	47	87	78
85	22	135	50	85	90

**Table 2.** Variations of receding contact angle, advancing contact angle, and tilt angles with drop volumes for *Alchemilla* leaf. All angles and volumes measured lie within an error of 2° and 1μL, respectively.

Tilt angle (°)	Volume (μL)	Contact angles (°)		Hysteresis (°)
		Advancing	Receding	
25	54	130	54	76
35	48	131	55	76
45	40	130	30	100
55	34	119	20	99
65	28	100	16	84
75	20	98	14	84
85	18	68	14	54

**Table 3.** Variations of advancing and receding contact angle for water-IPA drop on untreated Alchemilla leaf. All angles and volumes measured lie within an error of 2° and 1μL, respectively.

Tilt angle (°)	Volume (μL)	Contact angles (°)		Hysteresis (°)
		Advancing	Receding	
25	50	125	63	62
35	34	125	69	56
45	23	126	78	48
55	16	133	77	56
65	12	130	80	50
75	8	131	88	43
85	6	130	96	34

**Table 4.** Variations of advancing and receding contact angles for Teflon-coated Alchemilla leaf. All angles and volumes measured lie within an error of 2° and 1μL, respectively.

Tilt angle (°)	Volume (μL)	Contact angles (°)		Hysteresis (°)
		Advancing	Receding	
25	34	154	110	44
35	22	151	110	41
45	14	157	123	34
55	8	154	123	31
65	8	163	135	28
75	5	165	153	12
85	4	133	133	0

**Table 5.** Variations of advancing and receding contact angles for Hydrobead-coated *Alchemilla* leaf. All angles and volumes measured lie within an error of 2° and 1μL, respectively.

### 3.5. Condensation Experiment

Condensed water vapor settled on both, the fibers and the leaf face of the dry leaf. The interaction of water drops with fibers during condensation process observed in experiments can be discussed in two cases.

First case was when water drops condensed on a single fiber as represented in Figure 8.a. The small drops on the fiber merged together to form bigger drops (Figure 9.a). As more water drops formed on the fiber and merged with the existing drop, it grew bigger and heavier (Figure 9.a3 – 9.a4). Finally, it fell on the leaf face where it merged with drops that had been growing on the leaf face (Figure 9.a5).

Second case was when drops on multiple fibers merged to form a larger drop which remained suspended between the fibers, represented by Figure 8.b and Figure 8.c. In case observed in Figure 9.b, fiber bent due to the weight of drop on it and merged with drop on another fiber. Bigger drop stay suspended by maintaining contact with multiple fibers. Any two fibers parallel to, inclined towards or crossing each other can be found with drop suspended between them. As condensation continued, these drops got bigger and fell to the leaf face due to its increased weight. Near the margin of leaf where fibers had small inclination angles, bigger sized drops could remain suspended on fibers compared to near the center of leaf with fibers of larger inclination angles.

The drops on the leaf face merged with newer drop on the fibers as represented in Figure 9.c. Then, all drops settled on the leaf face as a result of each of the above cases merged with their neighboring drops to form even bigger drops (Figure 10.a).



Two other observations were made during condensation process, one was the movement of some fibers at the beginning and end of condensation process. The fiber marked by circle in Figure 10.b moved upwards when water began to condense on it. After evaporation these fibers moved back to their positions from before the start of condensation process. Another observation made was the strong pinning effect at the margin of the leaf due to close-packed fibers (Figure 10.c). The pinning of large drops at the margin was due to the reduced gap between fibers at the margin i.e. about  $1/4 - 1/3$  of the gap present elsewhere on the leaf.

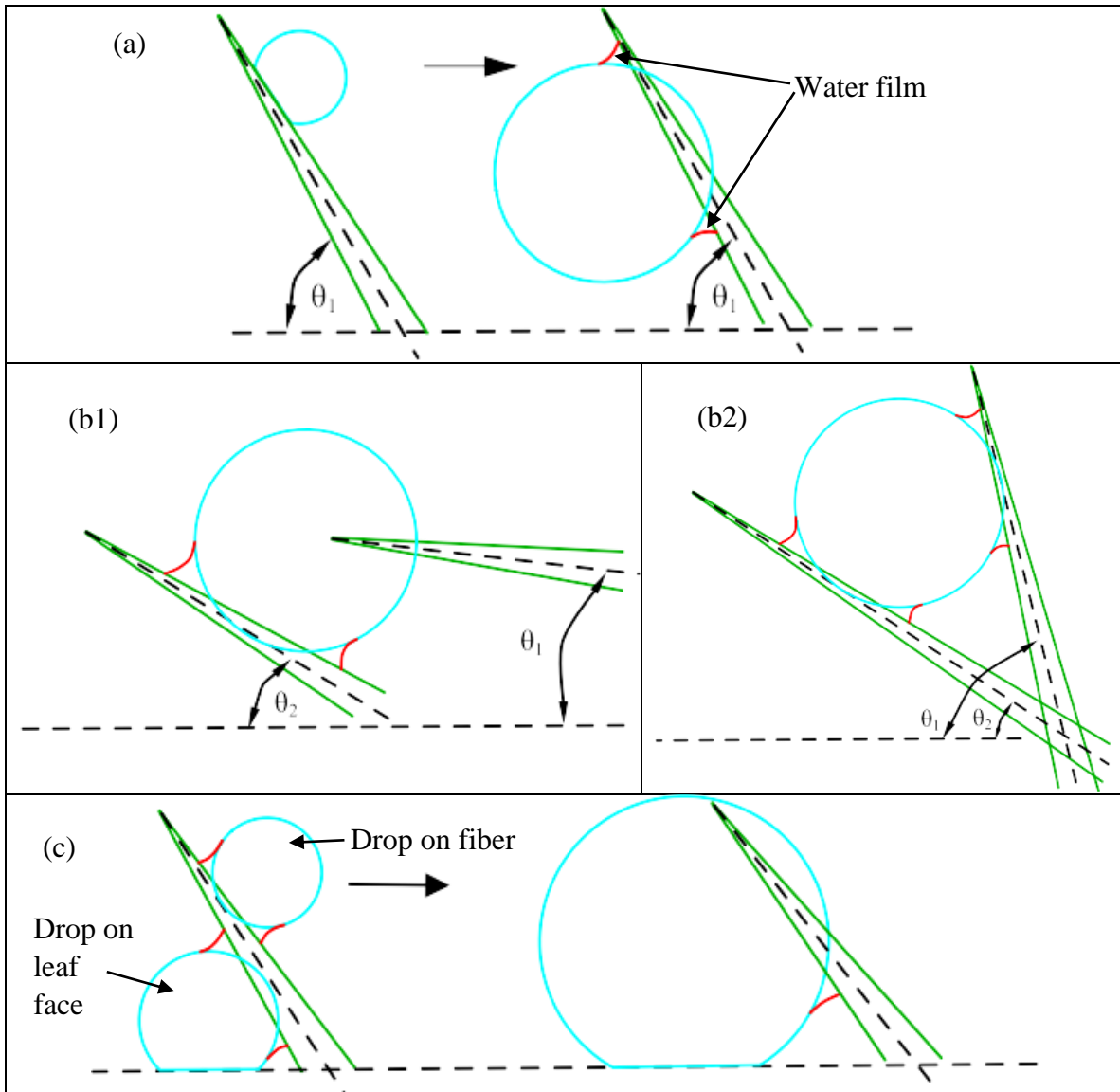


**Figure 8.** Illustration of cases in condensation processes: (a) drop on a single fiber, (b) drop suspended between multiple fibers and (c) merger of drop on fiber with drop on leaf face.

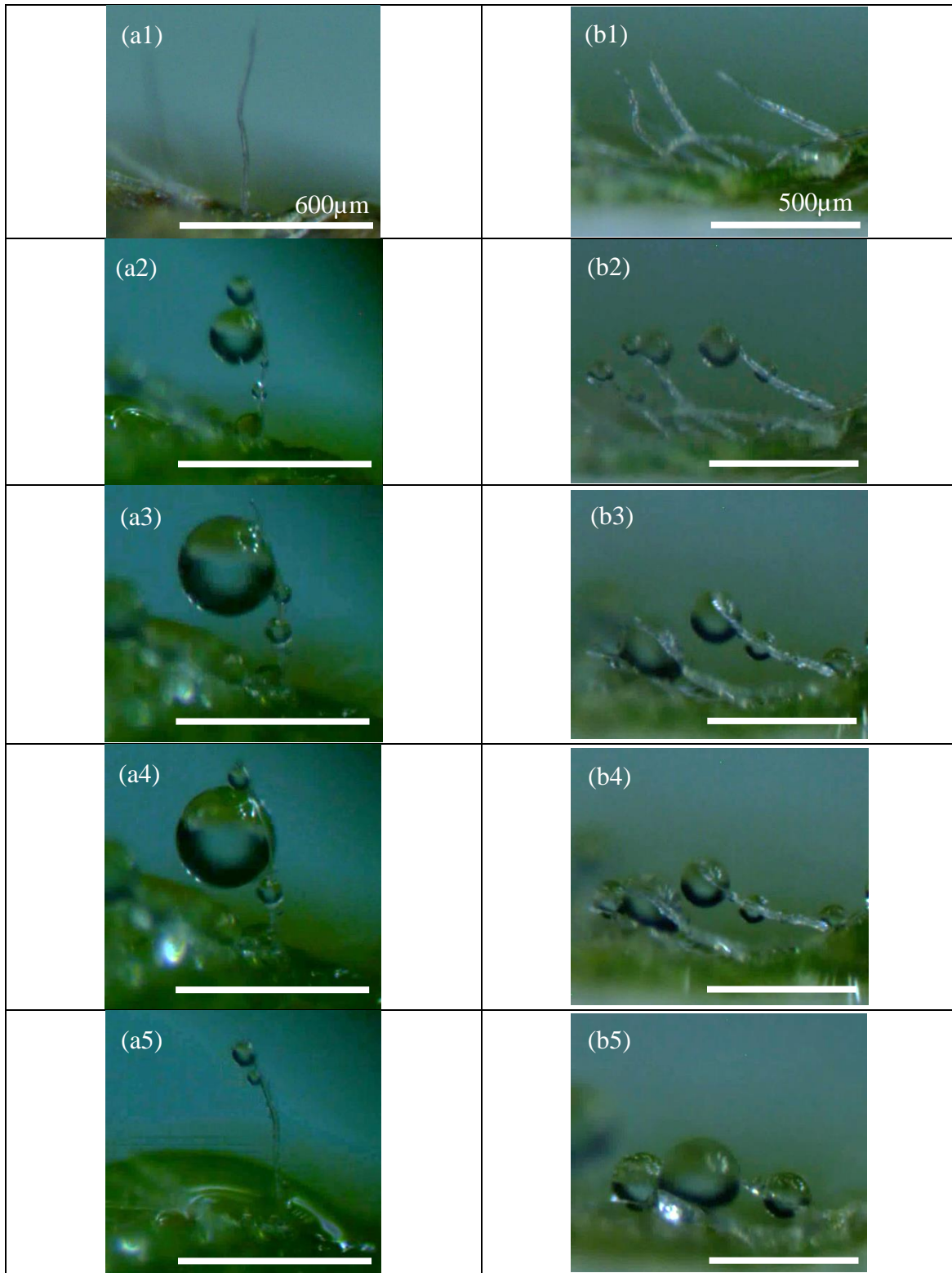


**Figure 9.** Condensation of drops on (a) a single fiber and (b) a group of fibers.

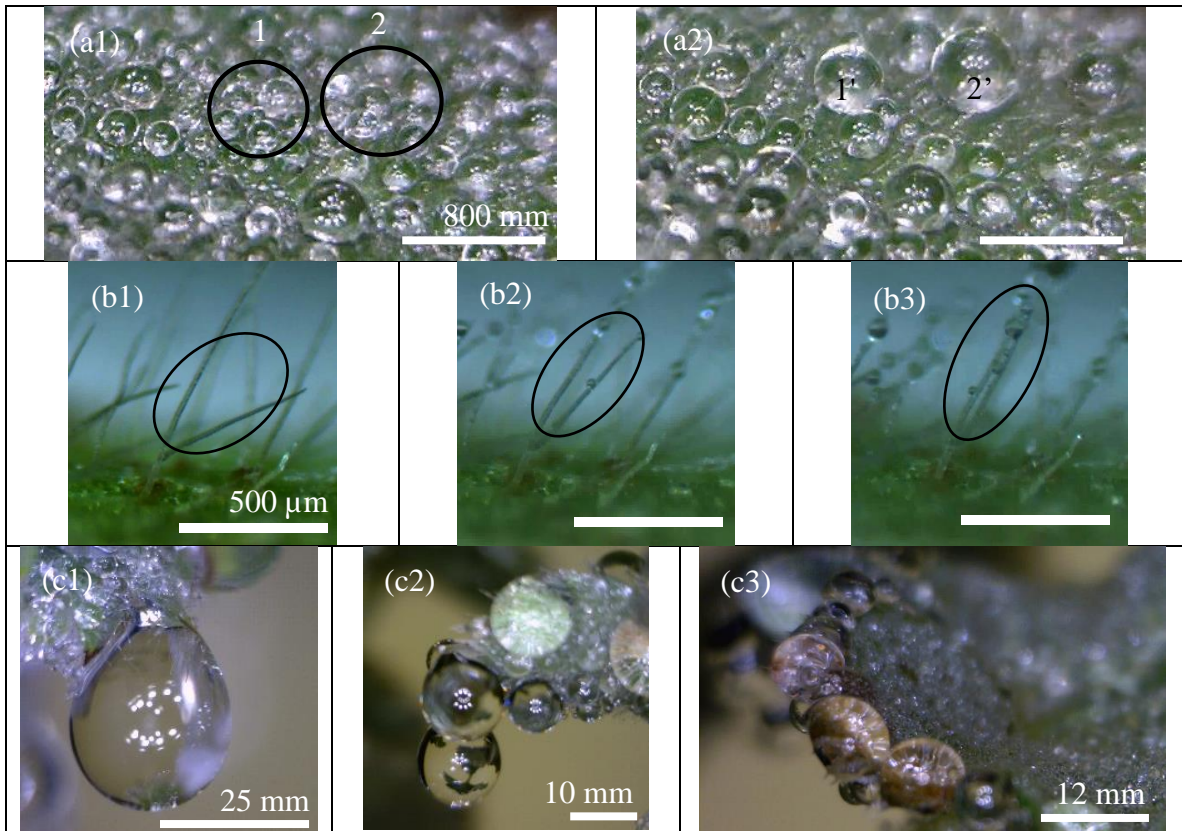


**Figure 10.** (a) The drops marked within circle 1 and 2 merged to form bigger drops 1' and 2', respectively. (b) Movement of fibers during a condensation process. (c) Pinning effect observed due to closely packed fibers at margin of a leaf.

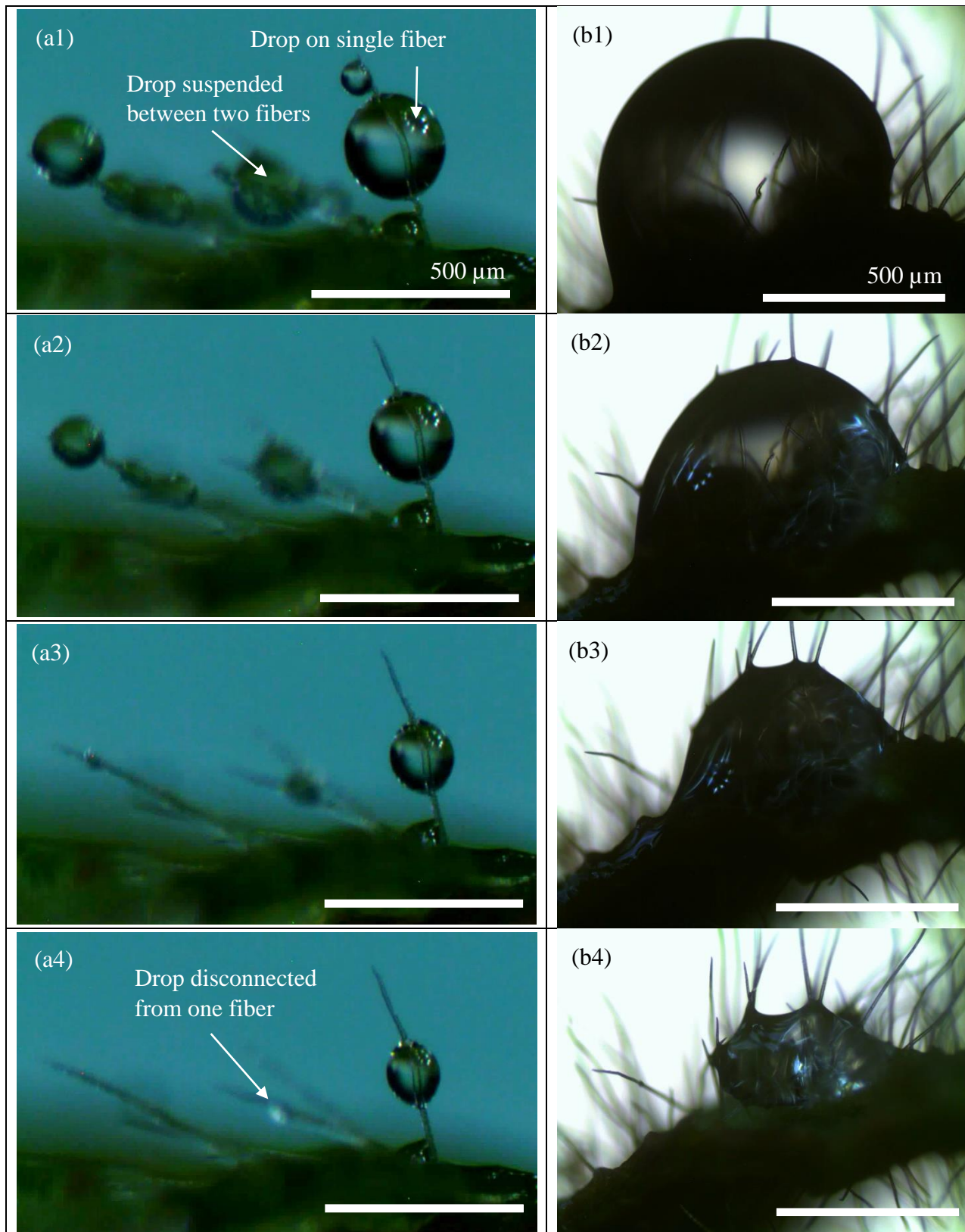
### 3.6. Evaporation Experiment

The large drops accumulated on the leaf because of condensation were kept under observation at room temp to slowly evaporate over time. The evaporation can be discussed in two cases depending on how the drop had interacted with the leaf during condensation process.

In first case we discuss drops settled on a fiber or bunch of fibers and having no contact with leaf face, which evaporated as shown in Figure 11.a. The drop shrunk, got disconnected from fibers and split to form smaller drops on each fiber. On a single fiber the drop became smaller until it had evaporated completely.

In the second case where drops started out, penetrated by many fibers and in contact with the leaf face, the evaporation process was as depicted in Figure 11.b. The drop reduced in size and lost its spherical curvature as soon as the drop became smaller and the fibers became visible above the drop. These drops then split into smaller drops (Figure 12.a) and continued evaporating. The drop shrunk and disconnected from more fibers and this continued until the drop was flattened to the face of the leaf.

The evaporation process was almost a complete reversal of the condensation process observed on the Achemilla leaf. The distortion in the profile of evaporating drop observed in Figure 11.b4 is also evidence to the hydrophilic nature of fibers.



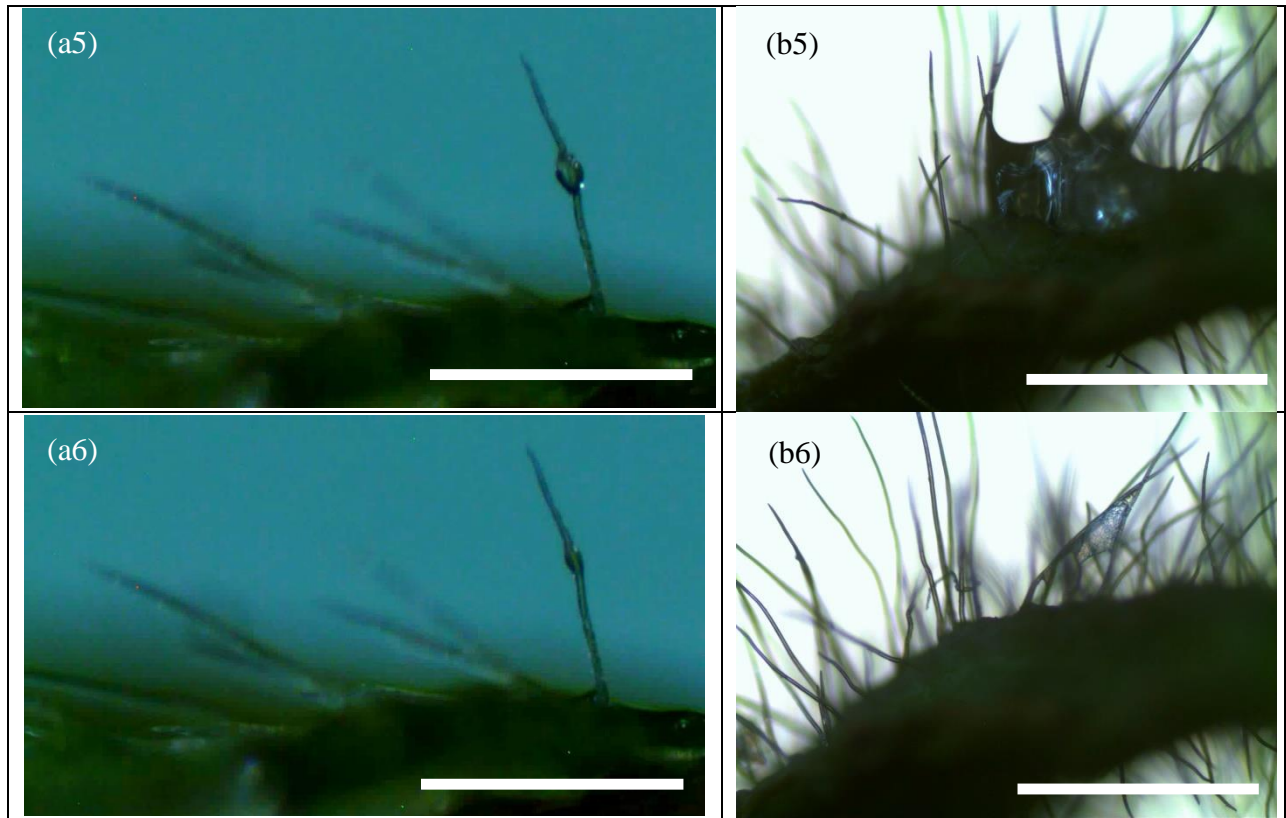


**Figure 11.** Evaporation of (a) drops on a single fiber and between two fibers and (b) a large drop having contact with multiple fibers and the leaf face.

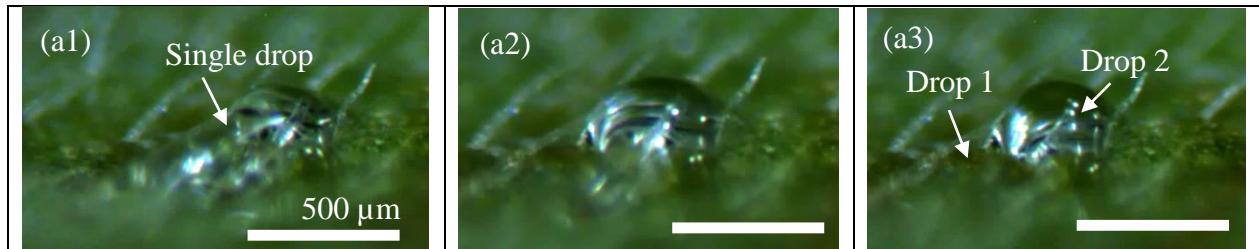


**Figure 12.** Splitting of a small drop during an evaporation process.

### 3.7. Rain Drop Experiment

A water drop when poured on the leaf using pipette was observed to have air pockets under it. These air pockets gave a bumpy appearance to the drop at the contact surface with leaf (Figure 13.a1). When the drop was big enough, it rolled down the leaf surface (Figure 13.a2). Air pockets were less likely to be present under a drop formed by condensation because, water drops settled on the leaf face during drop formation process (Figure 13.b1). The large condensed drops carried all the smaller drops in its path as it rolled down the leaf (Figure 13.b2). Therefore, in both cases when drop rolled off the leaf it left behind a dry leaf face.

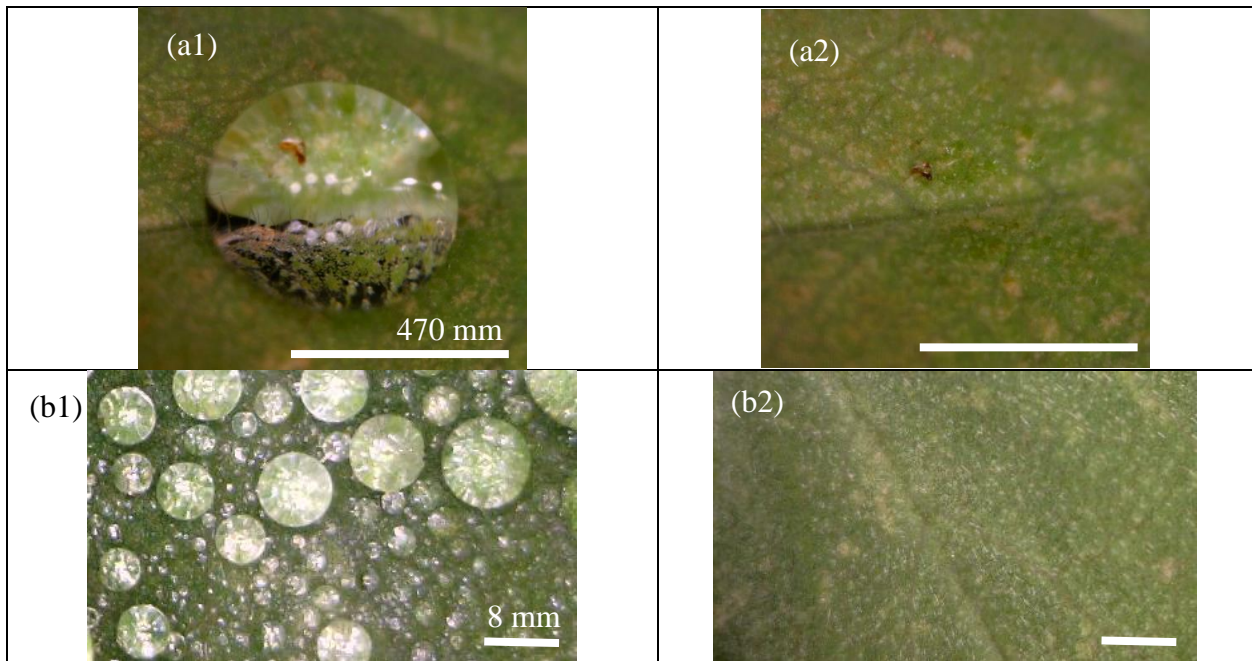


**Figure 13.** (a1) A water drop was poured on a leaf using a micropipette and (a2) no water residue was visibly seen after the drop rolled off the leaf. (b1) Water drops were condensed on the leaf and (b2) no water residue visibly seen after the larger drops carried the smaller drops as they rolled off the leaf.



### 3.8. Self-Cleaning Ability Experiment

The sample was set on bench tilted at  $60^\circ$  to allow easy rolling of water drop placed on the leaf. Particles of varying sizes (diameters of  $5 - 500 \mu\text{m}$ ) were randomly scattered on the leaf sample. Some particles settled on the fibers while others settled on the leaf face (Figure 14.a1 and 14.b1). Water drops were poured using a micropipette and allowed to roll over the particles. As the drop rolled down the leaf surface, it carried the particles with it leaving behind a clean leaf face (Figure 14.a2 and 14.b2). However, some particles of diameters smaller than  $10\mu\text{m}$  were not removed by the rolling drop.

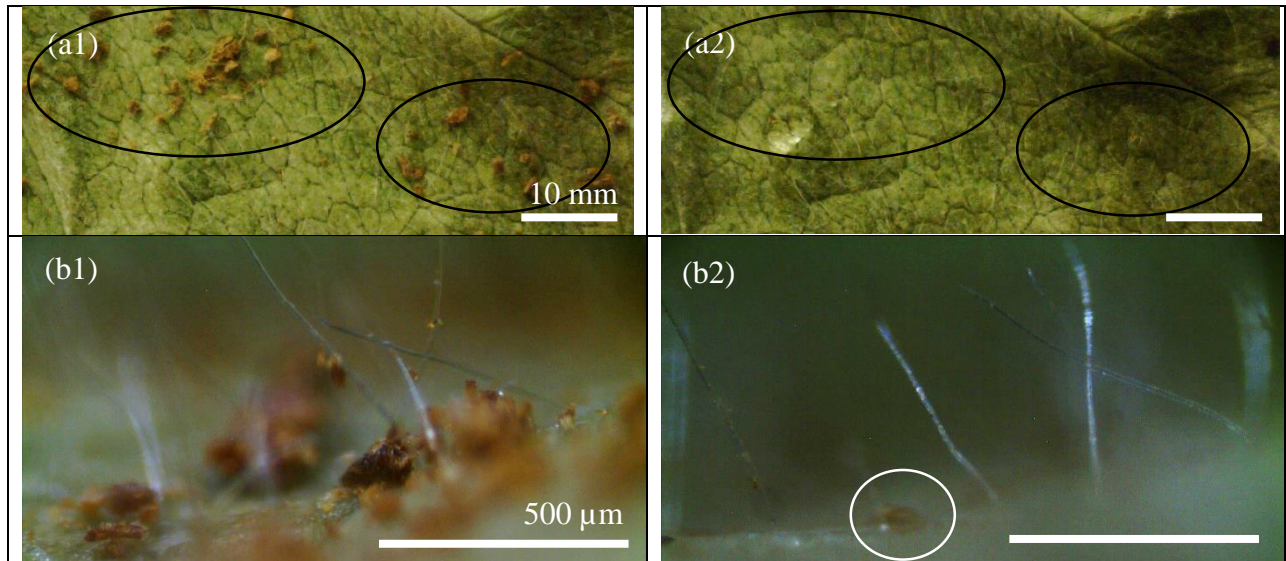


**Figure 14.** Optical images demonstrating self-cleaning ability: Top view of (a1) leaf with particles, and (a2) clean leaf face after drop rolled off. Side view of (b1) particles with diameters in the range of  $5 - 500 \mu\text{m}$ , and (b2) clean leaf face with traces of particles of diameters  $<10\mu\text{m}$  after the drop rolled off.

## Chapter 4

### Summary and Future Work

The inclined, hydrophilic fibers were experimentally observed and theoretically satisfy necessary conditions to allow water drops to stay suspended on the fibers in a meta-stable state. However, the fibers on penetrating the drop contributed largely towards pinning of water drops to the leaf. By turning the fibers hydrophobic we were able to reduce the contact angle hysteresis and pinning force. It should be possible to further reduce the contact angle hysteresis and pinning force by reducing the length of the fibers. The leaf has demonstrated self-cleaning ability, where it easily removed contaminants bigger than 10 $\mu$ m on the leaf surface. The leaf has also demonstrated self-drying ability through its ease of removal of small drops in the path of a large rolling drop.

This microstructure with optimization in the length and gap between fibers can be used in medical devices such as sweat collecting surface, where drops would stay pinned to the surface until ready for extraction. By mimicking the *Alchemilla* microstructure, we can also create a better cooling mechanism for microprocessors or other such devices.

## References

- [1] P. Wagner, "Quantitative assessment to the structural basis of water repellency in natural and technical surfaces", *Journal of Experimental Botany*, vol. 54, no. 385, pp. 1295-1303, 2003.
- [2] W. Barthlott and C. Neinhuis, "Purity of the sacred lotus, or escape from contamination in biological surfaces", *Planta*, vol. 202, no. 1, pp. 1-8, 1997.
- [3] A. Otten and S. Herminghaus, "How Plants Keep Dry: A Physicist's Point of View", *Langmuir*, vol. 20, no. 6, pp. 2405-2408, 2004.
- [4] M. Xiang, A. Wilhelm and C. Luo, "Existence and Role of Large Micropillars on the Leaf Surfaces of The President Lotus", *Langmuir*, vol. 29, no. 25, pp. 7715-7725, 2013.
- [5] C. Luo and M. Xiang, "Angle Inequality for Judging the Transition from Cassie–Baxter to Wenzel States When a Water Drop Contacts Bottoms of Grooves between Micropillars", *Langmuir*, vol. 28, no. 38, pp. 13636-13642, 2012.
- [6] N. Bernardino, V. Blickle and S. Dietrich, "Wetting of Surfaces Covered by Elastic Hairs", *Langmuir*, vol. 26, no. 10, pp. 7233-7241, 2010.
- [7] U. Mock, R. Förster, W. Menz and J. Rühle, "Towards ultrahydrophobic surfaces: a biomimetic approach", *Journal of Physics: Condensed Matter*, vol. 17, no. 9, pp. S639-S648, 2005.
- [8] Q. Wang, X. Yao, H. Liu, D. Quéré and L. Jiang, "Self-removal of condensed water on the legs of water striders", *Proceedings of the National Academy of Sciences*, vol. 112, no. 30, pp. 9247-9252, 2015.

- [9] Y. Chen, T. Lin and C. Martin, "Effects of guttation prevention on photosynthesis and transpiration in leaves of *Alchemilla mollis*", *Photosynthetica*, vol. 52, no. 3, pp. 371-376, 2014.
- [10] R. van der Veen, M. Hendrix, T. Tran, C. Sun, P. Tsai and D. Lohse, "How microstructures affect air film dynamics prior to drop impact", *Soft Matter*, vol. 10, no. 21, p. 3703, 2014.
- [11] M. Blow and J. Yeomans, "Superhydrophobicity on Hairy Surfaces", *Langmuir*, vol. 26, no. 20, pp. 16071-16083, 2010.
- [12] Kim, J.; Kim, C.-J. Nanostructured Surfaces for Dramatic Reduction of Flow Resistance in Drop-based Microfluidics, *Proc. IEEE Conf. MEMS*, Las Vegas, NV, Jan. 2002, 479-482.
- [13] de Gennes, P.-G.; Brochard-Wyart, F.; Quéré, D. Capillarity and Wetting Phenomena: Drops, Bubbles, Pearls, Waves. *Springer*, 2004.
- [14] Extrand, C.W.; Moon, S.I. When sessile drops are no longer small: transitions from spherical to fully flattened. *Langmuir* 2010, 26 (14), 11815.

## Biographical Information

Atul Kootathil completed his Bachelor of Science in Mechanical Engineering from Mumbai University in May 2012. His undergraduate project “Developing working model of Tesla Turbine using compressed air as working fluid” was highly appreciated by professors for developing a simple working turbine model. He has worked as a Trainee Design Engineer at HYDAC Pvt. Ltd. where he was responsible for various projects involving designing industrial oil filtration systems. He has been a Graduate student in Mechanical and Aerospace Department at UT Arlington since August 2014 and a part of Dr. Cheng Luo’s group since May 2015. His thesis project involved understanding the Alchemilla leaf microstructure and documenting the observations from experiments which highlights the parameters when attempting to mimetic its wetting behavior.